

Article

Hydrophilic Monomethyl Auristatin E Derivatives as Novel Candidates for the Design of Antibody-Drug Conjugates

Filip S. Ekholm ^{1,†}, Suvi-Katriina Ruokonen ^{1,†}, Marina Redón ¹, Virve Pitkänen ², Anja Vilkmann ², Juhani Saarinen ², Jari Helin ², Tero Satomaa ^{2,*} and Susanne K. Wiedmer ^{1,*}

¹ Department of Chemistry, University of Helsinki, PO Box 55, A. I. Virtasen aukio 1, FI 00014 Helsinki, Finland; filip.ekholm@helsinki.fi (F.S.E.); suvi.k.ruokonen@gmail.com (S.-K.R.); marina.redonmunoz@gmail.com (M.R.)

² Glykos Finland Ltd., Viikinkaari 6, 00790 Helsinki, Finland; virve.pitkanen@glykos.fi (V.P.); anja.vilkmann@glykos.fi (A.V.); juhani.saarinen@glykos.fi (J.S.); jari.helin@glykos.fi (J.H.)

* Correspondence: tero.satomaa@glykos.fi (T.S.); susanne.wiedmer@helsinki.fi (S.K.W.); Tel.: +358-9-3193-6340 (T.S.); +358-405-826-629 (S.K.W.)

† These authors contributed equally to this work.

Received: 28 October 2018; Accepted: 14 December 2018; Published: 24 December 2018



Abstract: Antibody-drug conjugates (ADCs) are promising state-of-the-art biopharmaceutical drugs for selective drug-delivery applications and the treatment of diseases such as cancer. The idea behind the ADC technology is remarkable as it combines the highly selective targeting capacity of monoclonal antibodies with the cancer-killing ability of potent cytotoxic agents. The continuous development of improved ADCs requires systematic studies on the nature and effects of warhead modification. Recently, we focused on the hydrophilic modification of monomethyl auristatin E (MMAE), the most widely used cytotoxic agent in current clinical trial ADCs. Herein, we report on the use of micellar electrokinetic chromatography (MEKC) for studying the hydrophobic character of modified MMAE derivatives. Our data reveal a connection between the hydrophobicity of the modified warheads as free molecules and their cytotoxic activity. In addition, MMAE-trastuzumab ADCs were constructed and evaluated in preliminary cytotoxic assays.

Keywords: antibody-drug conjugate; biopharmaceutical; cytotoxicity; hydrophobicity; micellar electrokinetic chromatography

1. Introduction

Natural science has witnessed many breakthroughs during the past decades. The new biological insights gained, the improved biochemical protocols and analytical tools developed, and the constant advances in chemical reaction technologies have paved the way for exciting and multidisciplinary research fields such as the field of antibody-drug conjugates (ADCs). ADCs are modern drug-delivery molecules that combine the selective targeting capabilities of monoclonal antibodies (mab) with the potent cytotoxicity displayed by toxic organic compounds [1,2]. The interest toward ADCs and the investments in ADC research have increased exponentially in recent years as a result of the U.S. Food and Drug Administration (FDA) approval of brentuximab vedotin (Adcetris®) in 2011 (for relapsed cases of Hodgkin's lymphoma and anaplastic large cell lymphoma) [3], trastuzumab emtansine (Kadcyla®) in 2013 (for human epidermal growth factor receptor 2 -positive metastatic breast cancer) [4], gemtuzumab ozogamicin (Mylotarg®) in 2017 (for acute myeloid leukemia) [5], and inotuzumab ozogamicin (Besponsa®) in 2017 (for acute lymphoblastic leukemia) [6].

The development of modern ADCs requires systematic research on antibodies, bioconjugation technologies, as well as information on the properties of the payload molecules and the characteristics of the end products. Recently, hydrophilic derivatization of payload molecules was reported to have beneficial effects on the overall properties of the ADCs, for example, on the therapeutic index and the pharmacokinetics [7,8]. In line with the current research trends, we developed an alternative strategy for increasing the hydrophilicity of the cytotoxic agents based on the incorporation of carbohydrates and we constructed a limited set of monomethyl auristatin E (MMAE)-carbohydrate hybrids [9].

MMAE (see the structure displayed in Figure 1) is an antineoplastic and antimetabolic drug that appears as the cytotoxic agent in at least sixteen ADCs which have progressed to clinical trials [10,11]. Among these is the ADC brentuximab vedotin, which is used in the treatment of relapsed cases of Hodgkin's lymphoma and anaplastic large cell lymphoma [3]. On a more general level, MMAE and other auristatins have become important cytotoxic agents for ADC development since they tolerate covalent structural modifications without substantial loss of cytotoxic activity. While this is beneficial, the hydrophobic nature of MMAE and especially current MMAE-linker conjugates is sub-optimal for the development of ADCs with high drug-to-antibody ratios. This is because the attachment of multiple drug-linker moieties of this kind may lead to devastating effects on the biocompatibility and pharmaceutical efficacy of the end products. These problems are reflected in the design of current ADCs where focus is placed on low drug-to-antibody ratios, typically in the range of 2–4. In addition, multi-drug resistant cancer cells tend to overexpress efflux pump proteins capable of removing hydrophobic cytotoxic agents from the intracellular environment, thus further diminishing their potential [12]. The incorporation of hydrophilic moieties in the cytotoxic agents or the payload molecules has been identified as a valid strategy for overcoming these challenges and circumventing issues related to unwanted aggregation and clearance of ADCs [13]. To date, hydrophilic linkers based on polyethylene glycol (PEG) [7], the sulfonate group [8], and carbohydrates [9] have been reported. We have previously focused on the inclusion of hydrophilic carbohydrates in the linker species and the cytotoxic agent due to their biocompatibility, pre-existing degradation routes, further derivatization possibilities, and, just as important, low cost.

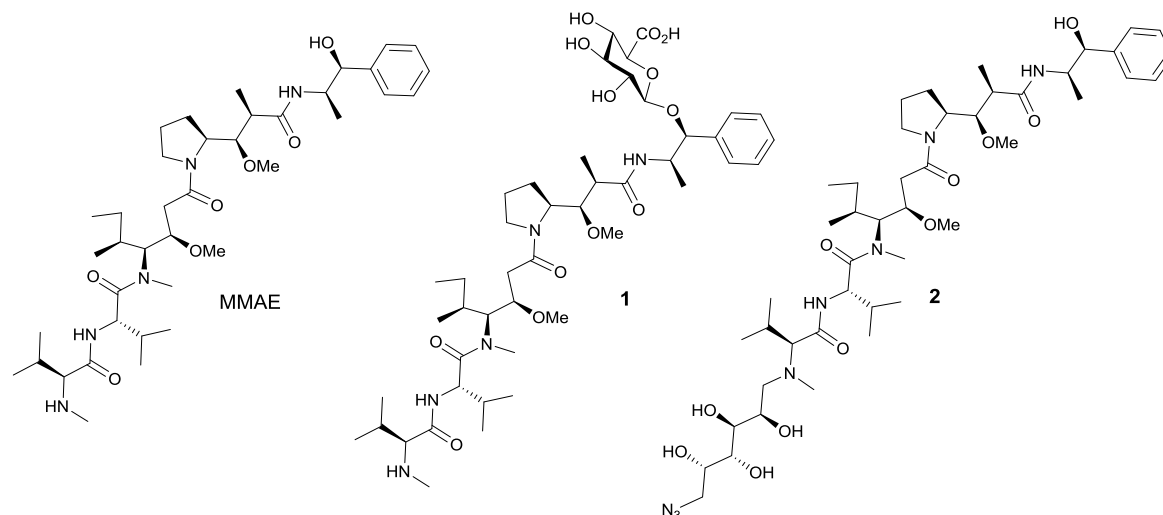


Figure 1. Chemical structures of the cytotoxic agents studied: from the left; monomethyl auristatin E (MMAE), 1 (β -D-glucuronyl-monomethylauristatin E, MMAU), and 2 (MMAE-glycolinker-substrate).

A thorough investigation of the change in the hydrophobic character was not included in the previous studies, even though it is important in understanding the nature of the modified molecules and the effects of the chosen strategy. Therefore, we continue our studies in this work by determining the relative hydrophobicities of MMAE and representatives of our own modified auristatins, namely, β -D-glucuronyl-monomethylauristatin E (MMAU, compound 1 in Figure 1) and

an MMAE-glycolinker-substrate (compound 2 in Figure 1), by micellar electrokinetic chromatography (MEKC) using sodium dodecyl sulfate and sodium cholate as surfactants. Furthermore, cytotoxic assays reveal an obvious connection between the hydrophobic properties of the warhead molecules and their corresponding cytotoxicity. Due to the mechanism by which ADCs function (internalization followed by the release of the cytotoxic agent), it was important to analyze the cytotoxic profiles of eventual end products in addition to those of the free warhead molecules. As a result, trastuzumab-auristatin derivatives, which can be used to treat HER2-positive breast cancer patients, were constructed and their cytotoxicities were screened.

2. Materials and Methods

2.1. Chemicals

Reagents and solvents were purchased from commercial sources. Reaction solvents were dried and distilled prior to use when necessary. All reactions containing moisture- and/or air-sensitive reagents were carried out under argon atmosphere.

2.2. Capillary Electrophoresis

A Hewlett Packard ^{3D}CE (Agilent, Waldbronn, Germany) instrument was used for all capillary electrophoresis (CE) runs. Uncoated fused silica capillary (length 30/38.5 cm) was obtained from Polymicro Technologies (Phoenix, AZ, USA) and the inner and outer diameters of the capillary were 50 µm and 375 µm, respectively. The separation voltage was 25 kV and the capillary cassette temperature was kept constant at 25 °C. Samples were injected at 10 mbar for 10 s. Thiourea (0.5 or 0.2 mM) was used as an electroosmotic flow (EOF) marker and 10 mM (ionic strength) sodium phosphate buffer at pH 7.4 was used as the background electrolyte (BGE) solution for CE runs. In MEKC studies, the surfactants were dispersed in the same BGE solution. New capillaries were preconditioned by rinsing for 15 min with 0.1 M sodium hydroxide, 15 min with water, and for 2–5 min with the CE or MEKC BGE solution. All runs were repeated at least five times.

2.3. Calculations of Retention Factors and Distribution Constants

The retention factor (*k*) in chromatography is a description of the time the sample component resides in the stationary phase (or pseudostationary phase, PSP) relative to the time it resides in the mobile phase. The expression states how much longer a sample component is retarded by the stationary phase than it would take to travel through the column or capillary with the velocity of the mobile phase. In the case of CE techniques, the stationary phase is either stationary as in capillary electrochromatography or pseudostationary as in electrokinetic capillary chromatography. The velocity of the mobile phase is based on the velocity of the EOF; however, external pressure assistance is also possible. In this work we used the EKC mode and here the retention factor describes the molar ratio of an analyte in a PSP and in an aqueous mobile phase, that is, ($\frac{n_{PSP}}{n_{aq}}$). From this expression it is obvious that the retention factor in EKC is dependent on the PSP concentration. In MEKC the retention factor can be calculated using Equation 1, when the effective electrophoretic mobility of the analyte under MEKC (μ_{MEKC}) and CE conditions (μ_0) is known, as well as the effective electrophoretic mobility of the micelles (μ_{PSP}):

$$k = \frac{u_{MEKC} - u_0}{u_{PSP} - u_{MEKC}} \quad (1)$$

An iteration procedure employing a homologous series of alkylbenzoates was used for estimating the μ_{PSP} , as previously reported [14,15]. The resulting values for 20 mM sodium dodecylsulfate (SDS) and for 20 mM SDS mixed with 40 mM sodium cholate (SC) (hereafter called 20/40 mM SDS/SC) were $-4.32E-08$ and $-4.06E-08 \text{ m}^2 \cdot \text{V}^{-1} \text{ s}^{-1}$, respectively.

The distribution constant (K_D) is the molar concentration ratio of an analyte between a pseudostationary phase and an aqueous phase and it can be calculated for systems with known phase ratios (ϕ) using Equation (2):

$$K_D = \frac{k}{\phi} \quad (2)$$

The phase ratio is the volume ratio of the pseudostationary phase and the aqueous phase in the fused silica capillary and it can be calculated from Equation (3):

$$\phi = \frac{V_{PSP}}{V_{aq}} = \frac{v_{spec, vol} \cdot M \cdot (c_{PSP} - CMC)}{1 - (v_{spec, vol} \cdot M \cdot (c_{PSP} - CMC))}, \quad (3)$$

where V_{PSP} and V_{aq} are the volumes of the pseudostationary phase and the aqueous phase in the capillary, respectively, $v_{spec, vol}$ is the partial specific volume, M is the molar mass, C_{PSP} is the total concentration of the surfactants, and CMC is the critical micelle concentration of the surfactants. The partial specific volumes of SDS and SC in phosphate buffer at pH 7.4 ($I = 10$ mM) were approximated to be close to the value in water at 25 °C and therefore values of 0.853 mL·g⁻¹ and 0.749 mL·g⁻¹, respectively, were used [16,17]. The partial specific volumes of the SDS/SC mixed micelles were estimated based on the used surfactant concentration ratios.

2.4. Determination of the Critical Micelle Concentration

For the phase ratio calculation, the surfactant CMCs in sodium phosphate buffer (pH 7.4, $I = 10$ mM) were determined with an optical contact angle meter using the pendant drop method (CAM 200 Optical Contact Angle Meter, Biolin Scientific, Espoo, Finland). Surface tensions of the surfactant solutions at different concentrations were determined by taking images of the pendant drops (4 drops/concentration, 20 frames/drop) with a CCD Video camera module and fitting a Young–Laplace equation to the frames using an Attension Theta Software (ver. 4.1.0. Biolin Scientific, Espoo, Finland). All measurements were repeated three times. The resulting CMCs for SDS and for the 20/40 SDS/SC mixture were 5.08 ± 0.24 and 6.00 ± 0.38 mM, respectively.

2.5. Preparation of Drug-Linker Compounds and Antibody-Drug Conjugates

MMAU and ϵ -maleimidocaproyl-L-valine-L-citrulline-paraaminobenzoyloxycarbonyl-paranitrophenyl (MC-Val-Cit-PABC-pNP) were prepared as described previously [18]. Interchain disulphide bridges of trastuzumab (Herceptin®, Roche, Espoo, Finland) were reduced with tris(2-carboxyethyl)phosphine (TCEP) and antibody drug-conjugates (ADCs) were synthesized by incubating 0.1 mM TCEP-reduced antibody with 50× molar excess of either MC-Val-Cit-PABC-MMAU or MC-Val-Cit-PABC-MMAE drug-linker compound as described by Satomaa et al. [18]. Non-conjugated drug-linkers were removed by repeated additions of formulation buffer (i.e., 5% mannitol-0.1% Tween-PBS) and centrifugation through Amicon Ultracel 30 K centrifugal filter (Merck KGaA, Darmstadt, Germany). In order to characterize the compounds, 30 µg of each ADC was digested with FabRICATOR enzyme (Genovis, Lund, Sweden) and analyzed with MALDI-TOF mass spectrometry using sinapinic acid matrix. After this, the drug-to-antibody ratios were calculated based on the observed relative intensities of the light chain fragments (LC) at m/z 24926 (LC + MMAU), Fab heavy chain fragments (Fab-HC) at m/z 29854 (Fab-HC + 3 MMAU), and Fc heavy chain fragments (Fc) at m/z 25227, 25389, and 25551 for differentially galactosylated fragments G0F-Fc, G1F-Fc, and G2F-Fc, respectively [18]. Both ADCs were similarly analyzed and found to have a drug-to-antibody ratio of 8.

2.6. Cytotoxicity Assay

In vitro cytotoxicity of the free payloads and ADCs was assayed similarly as described before [9]. Briefly, a human ovarian cancer cell line SKOV-3 (ATCC, Manassas, VA, USA) was seeded in cell culture medium onto 96-well plates and incubated overnight in a cell incubator. Dilution series of

free payloads and antibody-drug conjugates were applied to the cells in three parallel wells and the incubation was continued for 72 h. The viability of the cells was determined with PrestoBlue cell viability reagent (Life Technologies, Carlsbad, CA, USA) according to the manufacturer's instructions. The reagent was incubated with cells for 2–2.5 h and the absorbance was measured at 570 nm and 600 nm. IC₅₀ values were determined using curve fitting by nonlinear regression as the concentration of the drug that causes 50% inhibition of cell viability compared to maximum inhibition.

3. Results and Discussion

3.1. Micellar Electrokinetic Chromatography

The hydrophobic character of the cytotoxic agents displayed in Figure 1 was assessed using MEKC. The technique is excellent for the separation of charged and neutral compounds, and particularly for assessing the hydrophobicity of analytes. In MEKC the fused silica separation capillary is filled with amphiphilic surfactants, which are able to coalesce to form micelles at concentrations exceeding the critical micelle concentration [19–22]. Generally, liposomes and micelles are accepted models for interpreting the interactions between molecules and lipid bilayers, and therefore studying the interaction of the payload molecules in this system creates a simplified model for studying the interactions of the liberated drugs with cellular membranes. This is undoubtedly an important factor for antibody-drug conjugates as a whole. Therefore, the results of the MEKC studies generate more information than theoretically calculated partitioning coefficients or distribution constants (i.e., logP or logD values), especially from a biological perspective.

To evaluate the hydrophobicity of the cytotoxic agents MMAE, 1, and 2 (see Figure 1), the retention factors (*k*) and, moreover, the distribution constants (*K_D*) of the compounds were determined using negatively charged, highly hydrophobic SDS micelles, and a mixture of SDS and less hydrophobic SC micelles as pseudostationary phase in MEKC. Since the distribution constant of a compound in electrokinetic chromatography illustrates the strength of interaction between the compound and the pseudostationary phase, the value directly reflects the hydrophobicity of the compound; the higher the interaction, the higher is the distribution constant, and consequently, the higher is the hydrophobicity of the compound. The distribution constants, and the logarithm of the distribution constants, of the compounds using 20 mM SDS and 20/40 mM SDS/SC dispersions were calculated using Equations (1)–(3) (in the experimental section) and the values are shown in Figure 2. The corresponding electropherograms are shown in Figure 3.

SDS is the most frequently used surfactant in MEKC, and therefore the hydrophobicity of the auristatins was initially assessed using solely SDS micelles. From the experimental data it was obvious that the attachment of carbohydrates containing hydrophilic functional groups to MMAE decreased the hydrophobicity of the parent molecule in the order of MMAE > 2 > 1. In more detail, the *K_D* value decreased by 13% when the *N*-terminal of MMAE was modified by reductive amination with 6-deoxy-6-azido-D-galactose to give compound 2, whereas the decrease was 36% when the benzylic hydroxyl group in the norephedrine residue was modified by glycosylation with glucuronic acid to give compound 1. The distribution constants, that is, the relative hydrophobicity of the cytotoxic agents, are logical. The modification of the *N*-terminal of MMAE, which gives rise to 2, adds a hydrophilic tail to the molecule containing four hydroxyl groups. Surprisingly, this modification does not significantly alter the hydrophobic character of MMAE. The attachment of a glucuronic acid to the benzylic hydroxyl group of MMAE resulting in 1 is associated with a greater increase in hydrophilic character, especially compared to 2. This is logical since glucuronic acid contains a carboxylic acid functionality in addition to the hydroxyl groups. A 36% decrease in the distribution constant is considerable, especially since the structural variations between 1 and 2 are relatively small.

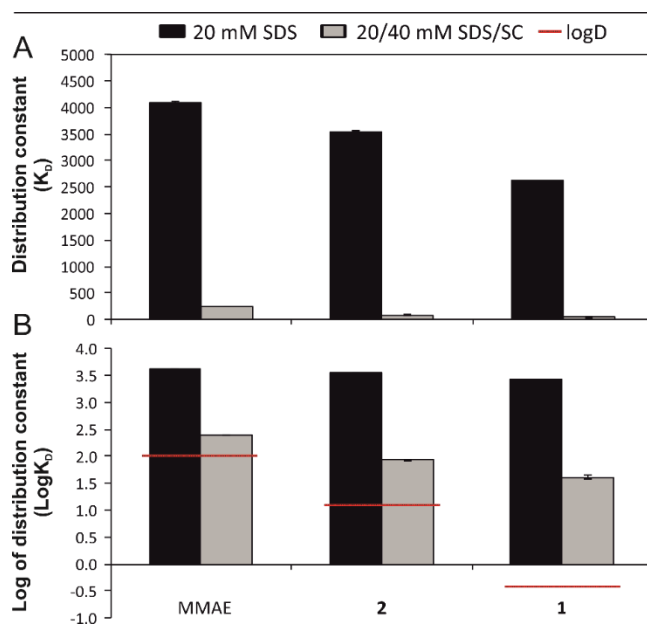


Figure 2. Distribution constants (displayed in 2A) and the logarithm of distribution constants (displayed in 2B) (including error bars) of MMAE, 1, and 2 by micellar electrokinetic chromatography (MEKC). Amounts of 20 mM sodium dodecyl sulfate (SDS) and 20 mM SDS mixed with 40 mM sodium cholate (SC) in sodium phosphate buffer (pH 7.4, I = 10 mM) were used as pseudostationary phases in MEKC. Thiourea was used as an EOF marker. Separation conditions were as follows: capillary length 30/38.5 cm; separation voltage 25 kV; capillary cassette temperature 25 °C; sample injection 10 s 10 mbar; UV detection at 200, 214, 238, and 254 nm. The inner and outer diameters of the capillary were 50 μm and 375 μm, respectively. The logD values represent the theoretically calculated distribution coefficients calculated by the ChemAxon software.

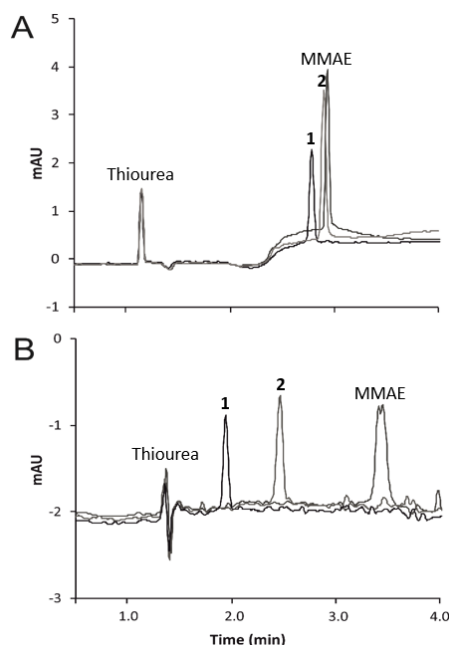


Figure 3. MEKC separation of the studied cytotoxic agents using (A) 20 mM SDS and (B) 20/40 mM of SDS/SC. The experimental conditions are similar to those in Figure 2.

The obtained results are consistent with theoretical octanol-water coefficients (logD) calculated by the ChemAxon software. The software estimates the logD values based on the structures of the compound as a function of pH, and the resulting logD values at pH 7.4 were 2.0, 1.1, and

−0.43 for MMAE, 2, and 1, respectively (shown as red lines in Figure 2). The $\log D$ values of the compounds follow the same order as the experimental $\log K_D$ values; however, the $\log D$ values were two to eight times lower and the differences between the $\log D$ values of the compounds were larger. The high experimentally determined $\log K_D$ values can be explained by the selection of SDS as the pseudostationary phase. SDS is a well-established anionic surfactant forming spherical micelles with a hydrophobic interior and a negatively charged hydrophilic exterior. These micelles are highly hydrophobic and, thus, the selectivity for neutral, highly hydrophobic, and fairly large compounds can be poor due to their nearly complete solubilization into the SDS micelles, resulting in co-migration of compounds [20,23–25]. In addition, SDS micelles are stronger hydrogen bond donors than 1-octanol and therefore they are expected to have strong interactions with hydrogen bond acceptor solutes like MMAE and its derivatives. Due to the poor selectivity of SDS micelles toward the used analytes, sodium cholate (SC), a biologically relevant anionic surfactant, was tested. SC is a common bile salt having a steroidal structure and it has been shown to be advantageous for separating hydrophobic compounds that cannot be separated by SDS [25–27].

Surprisingly, pure 40 mM SC micelles did not have any interaction with the cytotoxic agents (data not shown) and therefore different mixed micellar systems of SDS and SC were tested (20/10, 20/20, and 20/40 mM of SDS/SC). The addition of 10, 20, or 40 mM SC to the SDS solutions lowered the hydrophobicity of the SDS micelles in all cases, as witnessed by improved separations of the compounds with the optimal separation achieved by mixing 20 mM SDS with 40 mM SC. The compounds followed the same migration order as with pure SDS micelles ($1 > 2 > \text{MMAE}$), but the separation selectivity was much enhanced using a mixed SC and SDS system. With this pseudostationary phase, the hydrophobicity (K_D) decreased by 66% for compound 2 and by 84% for compound 1 (Figure 2B). Moreover, the $\log K_D$ values, obtained using the 20/40 mM SDS/SC mixture, were in a better correlation with the theoretical $\log D$ values than the values obtained using solely SDS as a pseudostationary phase (Figure 2B). One plausible explanation is that polar SC has a weaker solubilization power than SDS, and thus the SC/SDS mixture is a better model for biological systems [20].

3.2. Trastuzumab Conjugates and Cytotoxicity Assays

In our previous study, the cytotoxicities of MMAE ($IC_{50} = 4$ nM), 2 ($IC_{50} = 12$ nM), and an MMAE-glycolinker-cetuximab ADC ($IC_{50} = 9$ nM) were reported using HSC-2 head-and-neck squamous cell carcinoma cells [9]. It was rather surprising that the cytotoxicity displayed by MMAE was only marginally reduced when the *N*-terminal was modified with a glycolinker, since previous studies have established that an amide bond at the same site leads to the loss of cytotoxic activity [28]. While stable linkers have been found to improve the tolerability and antitumor activity in other state-of-the-art ADCs (e.g., the anti-HER2 ADC trastuzumab emtansine) [29], the glycolinker strategy failed to yield a superior ADC and the approach was not considered competitive enough.

Therefore, we decided to use a cleavable linker in this study. While a number of cleavable linkers exist (e.g., pH-sensitive linkers, enzyme targeting linkers) [25,26], we opted to use the cathepsin B cleavable linker valine-citrulline-*p*-aminocarbamate (Val-Cit-PABC) which is currently used in brentuximab vedotin [30]. Furthermore, we decided to evaluate the effects of the hydrophilic glucuronic acid residue at the hydroxyl group in the norephedrine residue of MMAE (the MMAE-glycolinker-substrate was thus not re-evaluated). In addition, it should be noted that the proteolysis of the Val-Cit-PABC-linker releases the warhead molecule as such instead of a conjugate thereof [31]. Therefore, it was important to start by evaluating the cytotoxicity of MMAE and MMAU (see Figure 1).

SKOV-3 ovarian carcinoma cells expressing the HER2 receptor protein were used, and the results are summarized in Figure 4. When evaluating the cytotoxicity using this cell line, MMAU was over three orders of magnitude less cytotoxic than MMAE when applied to the cell culture medium. It is therefore clear that an increase in the hydrophilic character of the MMAE derivatives is accompanied by

a decrease in the cytotoxic activity displayed. Based on these results alone, increasing the hydrophilicity and a steric bulk of the norephedrine-residue leads to a substantial decrease in the cytotoxicity of the parent molecule in contrast to the previous hydrophilic modification of the *N*-terminal. This may be related to the cellular uptake mechanism, which favors hydrophobic molecules, or to the binding mode by which the auristatins act at the tubulin receptor [32,33]. The first mechanism seems more plausible since we have established that MMAU displays an effective bystander effect when conjugated to an internalizing antibody such as an ADC [18]. This further indicates that the glucuronide is hydrolyzed in the intracellular milieu thus liberating the actual drug, namely, MMAE.

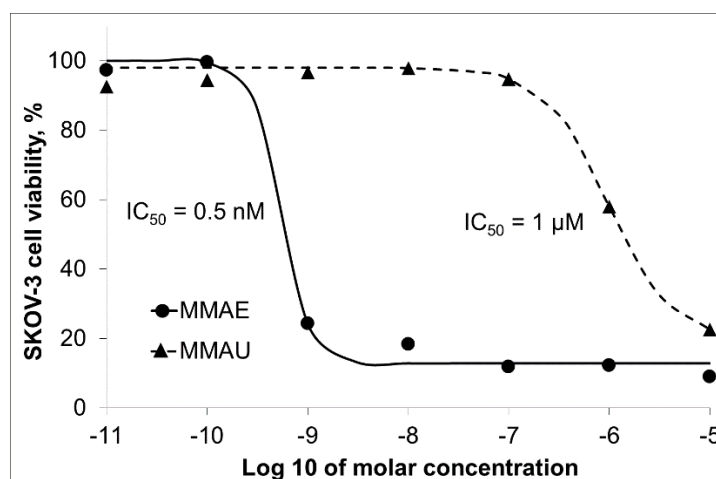
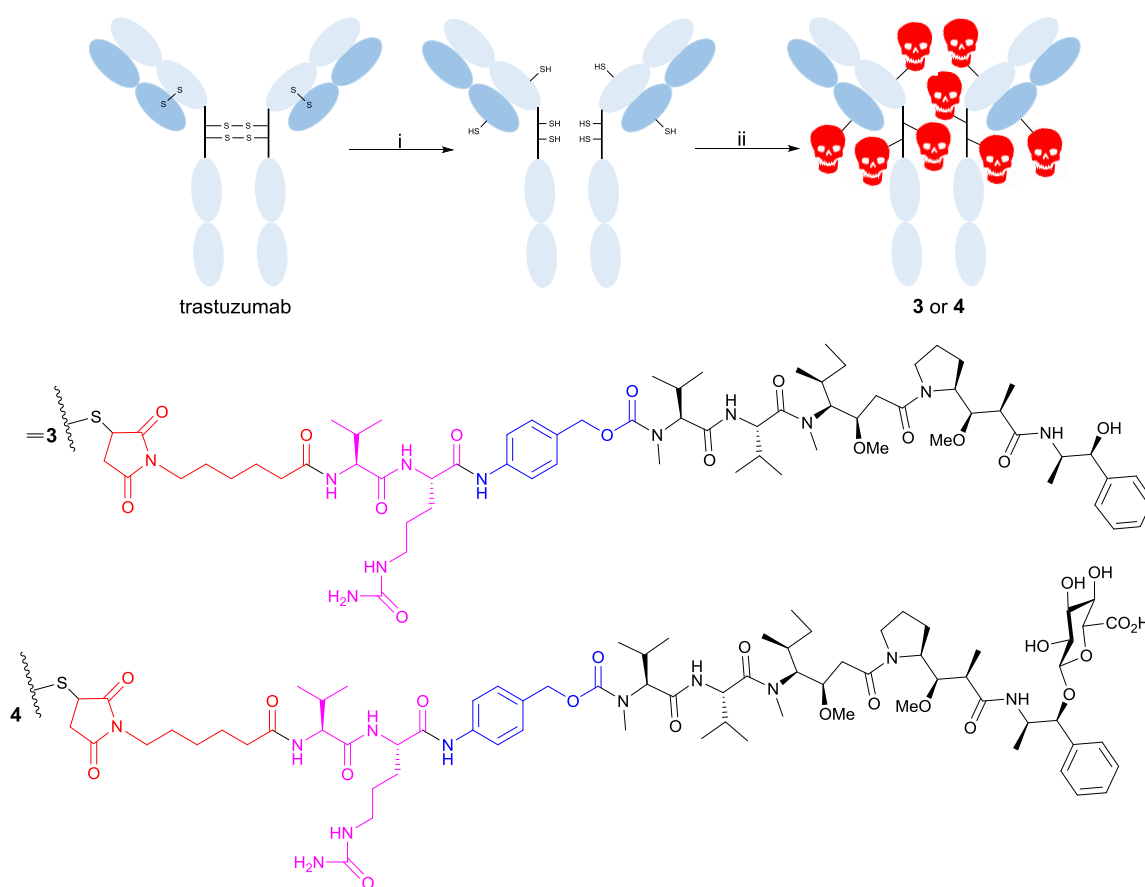


Figure 4. Cytotoxicity assays reveal that the hydrophobic payload MMAE is 2000-fold more cytotoxic against SKOV-3 ovarian cancer cells than MMAU.

In a traditional study on cytotoxic agents, these results would be conclusive; however, ADCs function by a different mechanism, that is, by the internalization of the entire ADC, followed by the release of the warhead molecule. Therefore, studying the properties of the cytotoxic agents alone does not provide the complete picture. As a result, we decided to conduct a preliminary study with ADCs featuring MMAE and MMAU. Since we used HER2-expressing ovarian cancer cells, we chose to use trastuzumab as the antibody. Trastuzumab was a logical choice since it is currently applied in both its naked form and as an ADC (trastuzumab emtansine) [34] in the treatment of HER2-positive breast cancer patients.

The strategy employed in the construction of the ADCs is displayed in Scheme 1 and described in detail elsewhere [18]. This resulted in compounds 3 and 4 being, respectively, the trastuzumab-MC-Val-Cit-PABC-MMAE derivative and the corresponding MMAU-trastuzumab conjugate. The preliminary cytotoxicity studies were conducted with an HER2-positive SKOV-3 cancer cell line (results summarized in Figure 5). Surprisingly, both compounds 3 and 4 displayed similar cytotoxicities with IC_{50} values in the pM-range (50–80 pM). The results are interesting, especially due to the large deviation in the cytotoxic activity of the free warheads. Taken together, the results indicate that the trastuzumab-MC-Val-Cit-PABC-MMAU derivative would be equally toxic as the corresponding MMAE-trastuzumab conjugate, however with a potentially decreased amount of off-site toxic side effects due to the reduced toxicity of the free drug.



Scheme 1. Schematic view of the construction of trastuzumab-MC-Val-Cit-PABC-auristatin ADCs. (i) TCEP reduction of interchain disulfides; (ii) thiol-maleimide conjugation of payload molecules. The warhead-linker conjugates are displayed below the conjugation route with different parts highlighted; the cytotoxic warhead molecule (black), the self-immolative PABC-spacer (blue), the cathepsin B cleavable Val-Cit-dipeptide (purple), and the MC conjugation site (red).

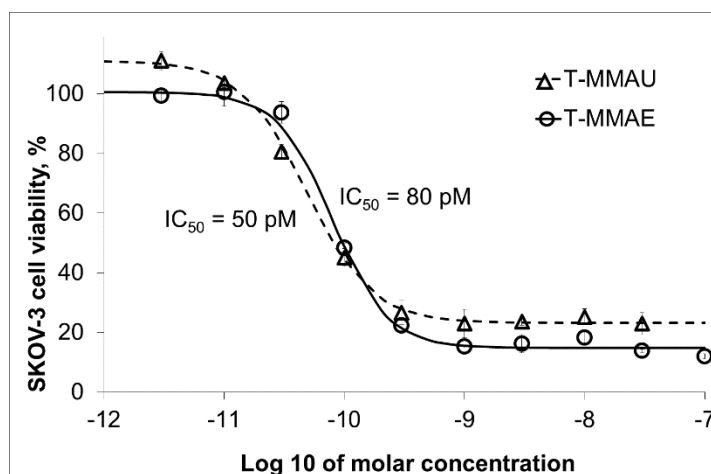


Figure 5. Trastuzumab antibody (T)-payload conjugates 3 and 4 have nearly comparable cytotoxicity against the HER2-expressing SKOV-3 cells, whereas they are between 10-fold (against MMAE) and 20,000-fold (against MMAU) more cytotoxic than the free payloads. In the assays, different concentrations of ADCs were applied to the cell culture medium and the cell viability was evaluated after 72 h incubation. The graph shows the average values of three parallel experiments. Error bars show the standard deviation.

These results prove that the construction of competitive ADCs can be achieved by the use of cytotoxic warheads that would normally be disregarded based on cytotoxicity assays alone. On a more fundamental level, the question that arises is why ADCs are not regularly screened for the delivery of hydrophilic agents across the cellular membrane, that is, molecules that would normally not pass the membrane. This is an area which requires further research and as our preliminary study on the cytotoxicity of the trastuzumab-auristatin ADCs shows, there is a significant potential for the development of novel ADCs with hydrophilic payload molecules. While we have focused on the use of carbohydrates as a means of increasing the hydrophilicity, other strategies have also been reported (e.g., the use of charged phosphate groups) [35]. It is clear that there is a need for more systematic studies with larger molecule libraries featuring hydrophilic and hydrophobic warhead molecules in order to provide detailed insights on the subject. Nonetheless, the benefits of carbohydrates are related to their specific lysosomal cleavage pathways in human cells, which provide an elegant way of adding hydrophilicity to the ADCs during the systemic distribution and localization in target tissues. Simultaneously, and using this pro-drug strategy, the fully active hydrophobic cytotoxic agent is generated after ADC internalization in target cells. In a recent follow-up study, we have shown that this concept is viable, since MMAU-ADCs show excellent cytotoxic activity against cancer cells both *in vitro* and *in vivo*, where complete eradication of tumors in xenografted mice was achieved [18].

4. Conclusions

MEKC was used for determining the relative hydrophobicities of modified auristatins. Optimal separation was achieved using a mixed micellar system of 20 mM SDS and 40 mM SC as the pseudostationary phase. The hydrophobicity of the auristatins decreased in the order of MMAE > compound 2 > compound 1, and the same pattern was identified in the cytotoxic assays where the cytotoxicity decreased in the same order.

Hydrophilic modification (attachment of a glucuronic acid residue) at the norephedrine residue of MMAE (compound 1; MMAU) was accompanied by a significant decrease in the cytotoxicity. The addition of a hydrophilic glycolinker at the *N*-terminal, on the other hand, had only a slight effect on the cytotoxicity (compound 2), which is an interesting observation since an amide bond at this position is known to render the auristatins close to non-toxic.

The preliminary cytotoxic evaluation of the trastuzumab-MC-Val-Cit-PABC-auristatin conjugates 3 and 4 revealed IC₅₀-values in the pM range. These values are comparable to other leading state-of-the-art ADCs. Furthermore, the MMAU-ADCs have certain advantages over the MMAE-ADCs, for example, prematurely cleaved linkers will be accompanied by less off-site harmful side effects due to the lower cytotoxicity of MMAU when compared to MMAE. Altogether, our results on the use of hydrophilic payload conjugates prove that novel opportunities exist for the future design of ADCs with previously neglected hydrophilic molecules.

Author Contributions: Conceptualization, F.S.E., S.-K.R., S.K.W.; Investigation, F.S.E., S.-K.R., M.R., V.P., A.V., J.S., J.H.; Resources, F.S.E., T.S., S.K.W.; Writing—Original Draft Preparation, F.S.E., S.-K.R., T.S., S.K.W.; Writing—Review and Editing, F.S.E., S.-K.R., S.K.W., T.S.; Visualization, F.S.E., S.-K.R., S.K.W.; Supervision, S.K.W.; Project Administration, F.S.E., S.K.W.; Funding Acquisition, F.S.E., S.K.W.

Funding: This research was funded by the Magnus Ehrnrooth Foundation (S.K.W.), the Ruth and Nils-Erik Stenbäck Foundation (F.S.E), The Finnish Society of Sciences and Letters (S.K.W.), and the Academy of Finland (S.K.W.; project number 266342).

Acknowledgments: Jesper Långbacka is acknowledged for assistance with the CMC measurements.

Conflicts of Interest: The authors declare no conflict of interest. The founding sponsors had no role in the design of the study; in the collection, analyses, or interpretation of data; in the writing of the manuscript; and in the decision to publish the results.

References

1. Schrama, D.; Reisfeld, R.A.; Becker, J.C. Antibody targeted drugs as cancer therapeutics. *Nat. Rev. Drug Discov.* **2006**, *5*, 147–159. [[CrossRef](#)] [[PubMed](#)]
2. Alley, S.C.; Okeley, N.M.; Senter, P.D. Antibody–drug conjugates: targeted drug delivery for cancer. *Curr. Opin. Chem. Biol.* **2010**, *14*, 529–537. [[CrossRef](#)] [[PubMed](#)]
3. Younes, A.; Bartlett, N.L.; Leonard, J.P.; Kennedy, D.A.; Lynch, C.M.; Sievers, E.L.; Forero-Torres, A. Brentuximab vedotin (SGN-35) for relapsed CD30-positive lymphomas. *N. Eng. J. Med.* **2010**, *363*, 1812–1821. [[CrossRef](#)] [[PubMed](#)]
4. Verma, S.; Miles, D.; Gianni, L.; Krop, I.E.; Welslau, M.; Baselga, J.; Pegram, M.; Oh, D.-Y.; Diéras, V.; Guardino, E. Trastuzumab emtansine for HER2-positive advanced breast cancer. *N. Eng. J. Med.* **2012**, *367*, 1783–1791. [[CrossRef](#)] [[PubMed](#)]
5. Rowe, J.M.; Löwenberg, B. Gemtuzumab ozogamicin in acute myeloid leukemia: a remarkable saga about an active drug. *Blood* **2013**, *121*, 4838–4841. [[CrossRef](#)] [[PubMed](#)]
6. Rytting, M.; Triche, L.; Thomas, D.; O'Brien, S.; Kantarjian, H. Initial experience with CMC-544 (inotuzumab ozogamicin) in pediatric patients with relapsed B-cell acute lymphoblastic leukemia. *Pediatr. Blood Cancer* **2014**, *61*, 369–372. [[CrossRef](#)] [[PubMed](#)]
7. Lyon, R.P.; Bovee, T.D.; Doronina, S.O.; Burke, P.J.; Hunter, J.H.; Neff-LaFord, H.D.; Jonas, M.; Anderson, M.E.; Setter, J.R.; Senter, P.D. Reducing hydrophobicity of homogeneous antibody–drug conjugates improves pharmacokinetics and therapeutic index. *Nat. Biotechnol.* **2015**, *33*, 733–735. [[CrossRef](#)] [[PubMed](#)]
8. Zhao, R.Y.; Wilhelm, S.D.; Audette, C.; Jones, G.; Leece, B.A.; Lazar, A.C.; Goldmacher, V.S.; Singh, R.; Kovtun, Y.; Widdison, W.C. Synthesis and evaluation of hydrophilic linkers for antibody–maytansinoid conjugates. *J. Med. Chem.* **2011**, *54*, 3606–3623. [[CrossRef](#)] [[PubMed](#)]
9. Ekholm, F.S.; Pynnönen, H.; Vilkmán, A.; Pitkänen, V.; Helin, J.; Saarinen, J.; Satomaa, T. Introducing glycolinkers for the functionalization of cytotoxic drugs and applications in antibody–drug conjugation chemistry. *ChemMedChem* **2016**, *11*, 2501–2505. [[CrossRef](#)]
10. Johansson, M.P.; Maaheimo, H.; Ekholm, F.S. New insight on the structural features of the cytotoxic auristatins MMAE and MMAF revealed by combined NMR spectroscopy and quantum chemical modelling. *Sci. Rep.* **2017**, *7*, 15920. [[CrossRef](#)] [[PubMed](#)]
11. Rostami, S.; Qazi, I.; Sikorski, R. The clinical landscape of antibody–drug conjugates. *ADC Rev.* **2014**. [[CrossRef](#)]
12. Barok, M.; Joensuu, H.; Isola, J. Trastuzumab emtansine: mechanisms of action and drug resistance. *Breast Cancer Res.* **2014**, *16*, 209. [[CrossRef](#)] [[PubMed](#)]
13. Hamblett, K.J.; Senter, P.D.; Chace, D.F.; Sun, M.M.; Lenox, J.; Cervený, C.G.; Kissler, K.M.; Bernhardt, S.X.; Kopcha, A.K.; Zabinski, R.F. Effects of drug loading on the antitumor activity of a monoclonal antibody drug conjugate. *Clin. Cancer Res.* **2004**, *10*, 7063–7070. [[CrossRef](#)] [[PubMed](#)]
14. Bushey, M.M.; Jorgenson, J.W. Separation of dansylated methylamine and dansylated methyl-d3-amine by micellar electrokinetic capillary chromatography with methanol-modified mobile phase. *Anal. Chem.* **1989**, *61*, 491–493. [[CrossRef](#)]
15. Laine, J.; Lokajová, J.; Parshintsev, J.; Holopainen, J.M.; Wiedmer, S.K. Interaction of a commercial lipid dispersion and local anesthetics in human plasma: Implications for drug trapping by “lipid-sinks”. *Anal. Bioanal. Chem.* **2010**, *396*, 2599–2607. [[CrossRef](#)] [[PubMed](#)]
16. Ahlstrom, D.M.; Hoyos, Y.M.; Arslan, H.; Akbay, C. Binary mixed micelles of chiral sodium undecenyl leucinate and achiral sodium undecenyl sulfate: I. Characterization and application as pseudostationary phases in micellar electrokinetic chromatography. *J. Chromatogr. A* **2010**, *1217*, 375–385. [[CrossRef](#)] [[PubMed](#)]
17. González-Gaitano, G.; Compostizo, A.; Sánchez-Martín, L.; Tardajos, G. Speed of sound, density, and molecular modeling studies on the inclusion complex between sodium cholate and β -cyclodextrin. *Langmuir* **1997**, *13*, 2235–2241. [[CrossRef](#)]
18. Satomaa, T.; Pynnönen, H.; Vilkmán, A.; Kotiranta, T.; Pitkänen, V.; Heiskanen, A.; Herpers, B.; Price, L.S.; Helin, J.; Saarinen, J. Hydrophilic Auristatin Glycoside Payload Enables Improved Antibody–Drug Conjugate Efficacy and Biocompatibility. *Antibodies* **2018**, *7*, 15. [[CrossRef](#)]
19. Terabe, S.; Otsuka, K.; Ichikawa, K.; Tsuchiya, A.; Ando, T. Electrokinetic separations with micellar solutions and open-tubular capillaries. *Anal. Chem.* **1984**, *56*, 111–113. [[CrossRef](#)]

20. Nishi, H.; Terabe, S. Micellar electrokinetic chromatography perspectives in drug analysis. *J. Chromatogr. A* **1996**, *735*, 3–27.
21. Silva, M. Micellar electrokinetic chromatography: A review of methodological and instrumental innovations focusing on practical aspects. *Electrophoresis* **2013**, *34*, 141–158. [[CrossRef](#)] [[PubMed](#)]
22. Deeb, S.E.; Dawwas, H.A.; Gust, R. Recent methodological and instrumental development in MEKC. *Electrophoresis* **2013**, *34*, 1295–1303. [[CrossRef](#)] [[PubMed](#)]
23. Ji, A.J.; Nunez, M.F.; Machacek, D.; Ferguson, J.E.; Iossi, M.F.; Kao, P.C.; Landers, J.P. Separation of urinary estrogens by micellar electrokinetic chromatography. *J. Chromatogr. B* **1995**, *669*, 15–26. [[CrossRef](#)]
24. Jumppanen, J.H.; Wiedmer, S.K.; Siren, H.; Riekkola, M.L.; Haario, H. Optimized Separation of 7 Corticosteroids by Micellar Electrokinetic Chromatography. *Electrophoresis* **1994**, *15*, 1267–1272. [[CrossRef](#)] [[PubMed](#)]
25. Wiedmer, S.K.; Jumppanen, J.H.; Haario, H.; Riekkola, M.L. Optimization of selectivity and resolution in micellar electrokinetic capillary chromatography with a mixed micellar system of sodium dodecyl sulfate and sodium cholate. *Electrophoresis* **1996**, *17*, 1931–1937. [[CrossRef](#)] [[PubMed](#)]
26. Cole, R.O.; Sepaniak, M.J.; Hinze, W.L.; Gorse, J.; Oldiges, K. Bile salt surfactants in micellar electrokinetic capillary chromatography: application to hydrophobic molecule separations. *J. Chromatogr. A* **1991**, *557*, 113–123. [[CrossRef](#)]
27. Yang, S.; Bumgarner, J.G.; Kruk, L.F.; Khaledi, M.G. Quantitative structure-activity relationships studies with micellar electrokinetic chromatography influence of surfactant type and mixed micelles on estimation of hydrophobicity and bioavailability. *J. Chromatogr. A* **1996**, *721*, 323–335. [[CrossRef](#)]
28. Doronina, S.O.; Mendelsohn, B.A.; Bovee, T.D.; Cervený, C.G.; Alley, S.C.; Meyer, D.L.; Oflazoglu, E.; Toki, B.E.; Sanderson, R.J.; Zabinski, R.F. Enhanced activity of monomethylauristatin F through monoclonal antibody delivery: effects of linker technology on efficacy and toxicity. *Bioconjug. Chem.* **2006**, *17*, 114–124. [[CrossRef](#)]
29. Lambert, J.M.; Chari, R.V. Ado-trastuzumab Emtansine (T-DM1): an antibody–drug conjugate (ADC) for HER2-positive breast cancer. *J. Med. Chem.* **2014**, *57*, 6949–6964. [[CrossRef](#)]
30. Alley, S.C.; Benjamin, D.R.; Jeffrey, S.C.; Okeley, N.M.; Meyer, D.L.; Sanderson, R.J.; Senter, P.D. Contribution of linker stability to the activities of anticancer immunoconjugates. *Bioconjug. Chem.* **2008**, *19*, 759–765. [[CrossRef](#)]
31. Senter, P.D.; Sievers, E.L. The discovery and development of brentuximab vedotin for use in relapsed Hodgkin lymphoma and systemic anaplastic large cell lymphoma. *Nat. Biotechnol.* **2012**, *30*, 631–637. [[CrossRef](#)] [[PubMed](#)]
32. Waight, A.B.; Bargsten, K.; Doronina, S.; Steinmetz, M.O.; Sussman, D.; Protá, A.E. Structural basis of microtubule destabilization by potent auristatin anti-mitotics. *PLoS ONE* **2016**, *11*, e0160890. [[CrossRef](#)] [[PubMed](#)]
33. Wang, Y.; Benz, F.W.; Wu, Y.; Wang, Q.; Chen, Y.; Chen, X.; Li, H.; Zhang, Y.; Zhang, R.; Yang, J. Structural Insights into the Pharmacophore of Vinca Domain Inhibitors of Microtubules. *Mol. Pharmacol.* **2016**, *89*, 233–242. [[CrossRef](#)] [[PubMed](#)]
34. Phillips, G.D.L.; Li, G.; Dugger, D.L.; Crocker, L.M.; Parsons, K.L.; Mai, E.; Blättler, W.A.; Lambert, J.M.; Chari, R.V.; Lutz, R.J. Targeting HER2-positive breast cancer with trastuzumab-DM1, an antibody–cytotoxic drug conjugate. *Cancer Res.* **2008**, *68*, 9280–9290. [[CrossRef](#)] [[PubMed](#)]
35. Zhao, R.Y.; Erickson, H.K.; Leece, B.A.; Reid, E.E.; Goldmacher, V.S.; Lambert, J.M.; Chari, R.V. Synthesis and biological evaluation of antibody conjugates of phosphate prodrugs of cytotoxic DNA alkylators for the targeted treatment of cancer. *J. Med. Chem.* **2012**, *55*, 766–782. [[CrossRef](#)] [[PubMed](#)]

